

1 Title page

2

3 Computational modeling of the Hybrid procedure in hypoplastic left heart syndrome: a comparison of
4 zero-dimensional and three-dimensional approach.

5

6 Authors

7 Andrew Young^{a,b}

8 Terry Gourlay^a

9 Sean McKee^b

10 Mark HD Danton^{a,c}

11

12 ^aDepartment of Biomedical Engineering, University of Strathclyde, Glasgow, Scotland UK

13 ^bDepartment of Mathematics and Statistics, University of Strathclyde, Glasgow, Scotland UK

14 ^cDepartment of Cardiac Surgery, Royal Hospital for Sick Children, Glasgow, Scotland UK

15

16 Corresponding Author

17

18 Mark HD Danton

19 Department of Cardiac Surgery

20 Royal Hospital for Sick Children

21 Glasgow

22 Scotland, UK

23 G3 8SJ

24 danton.mark@googlemail.com

25 Tel +44 141 201 0000

26

27

28 Abstract

29 Previous studies have employed generic 3D-multiscale models to predict haemodynamic effects of the
30 hybrid procedure in hypoplastic left heart syndrome. Patient-specific models, derived from image data,
31 may allow a more clinically relevant model. However, such models require long computation times and
32 employ internal pulmonary artery band [d_{int}] dimension, which limits clinical application. Simpler,
33 zero-dimensional models utilize external PAB diameters [d_{ext}] and provide rapid analysis, which may
34 better guide intervention. This study compared 0-D and 3-D modeling from a single patient dataset and
35 investigated the relationship d_{int} versus d_{ext} and hemodynamic outputs of the two models. Optimum
36 oxygen delivery defined at $d_{\text{int}} = 2$ mm corresponded to $d_{\text{ext}} = 3.1$ mm and 3.4 mm when models were
37 matched for cardiac output or systemic pressure, respectively. 0-D and 3-D models when matched for
38 PAB dimension produced close equivalence of hemodynamics and ventricular energetics.

39 From this study we conclude that 0-D model can provide a valid alternative to 3D-multiscale in the

40 Hybrid-HLHS circulation

41

42 Abbreviations

43 HLHS = Hypoplastic left heart syndrome

44 0-D = zero-dimensional

45 3-D = three-dimensional

46 Q_p = pulmonary flow

47 Q_s = systemic flow

48 PAB = pulmonary artery band

49 PDA = patent Ductus Arteriosus

50 d_{int} = internal diameter of PAB

51 d_{ext} = external diameter of PAB

52

53 Introduction

54

55 In hypoplastic left heart syndrome there is developmental failure of left heart structure and the
56 right ventricle must supply both systemic and pulmonary circulations. This is achieved in the
57 newborn with the Hybrid procedure which stabilizes the circulation by regulating the correct
58 flow distribution between the pulmonary and systemic circulation, $Q_P:Q_S$ using surgically
59 placed bilateral PA bands. A stent placed in the PDA permits unrestricted blood flow from the
60 single ventricle to the systemic circulation. [Fig.1]. Defining the correct PAB dimension is critical
61 as this determines ventricular workload, systemic oxygen delivery and patient outcome. During Hybrid
62 procedure the PAB dimension is empirically based on patient's body weight and calibrated during
63 surgery to achieve desired systemic oxygen saturations and pressure. Because the method is
64 imprecise and the clinical parameters used to inform the PAB size reflect poorly the ventricular
65 workload and circulation, the condition still carries a significant risk [1,2].

66 Computational models have been used to inform congenital circulations and surgical intervention
67 including Norwood and Hybrid procedure [3-7]. They have provided a theoretical analysis of how the
68 circulation might be influenced by varying PAB dimension, stent size and aortic obstruction.

69 Multiscale models construct an idealized, generic 3-D geometry to represent the surgical region from
70 which regional flow profiles can be calculated. Alternatively the geometry of the surgical region can be
71 obtained from the patient's image dataset, thus providing a patient-specific model. Such models define
72 PAB and stent-PDA size by internal luminal dimensions which is in contrast to the surgical
73 procedure, being based on calibration of the external PAB dimension [1,2]. This difference in
74 quantifying PAB dimension and the fact that these models are computationally demanding limit their
75 clinical application.

76 An alternative approach is to represent the surgical region by lumped parameter method. Using
77 regional pressure data obtained during surgery or cardiac catheterization parameters of resistance can
78 be defined and related to flow [8,9]. 0-D models because of their simplicity can provide fast and
79 reliable solutions and potentially greater clinical application compared with the 3D-multiscale
80 approach. However simplicity should not compromise accurate description of the physiology.

81 In this study we compared 0-D and 3D-multiscale patient-specific models of the surgical region
82 constructed from a single patient dataset. This allowed a comparative analysis of the predicted
83 physiological outcomes of the two modeling approaches. Furthermore by comparing the models under

84 equivalent hemodynamic conditions, corresponding external and internal PA band diameters, defining
85 the PAB dimension in the 0-D and 3-D models respectively, were determined.

86

87 Methods

88 The analysis was based on a 3kg patient with HLHS with aortic atresia. Hybrid palliation included
89 3mm bilateral PA bands and 10mm PDA stent.

90 The surgical region [main pulmonary artery, PABs, PDA-ductal stent] was represented by either
91 equations-based 0-D model or 3-D model derived from the patient's CT scan. The remaining
92 cardiovascular system was described as lumped parameter network [LPN]. In order to compute the
93 entire circulation [surgical region +LPN] with the 0-D model the equations representing the surgical
94 region were incorporated as part of the LPN [fig 2a] whereas in the multiscale model the 3D geometry
95 region was coupled to LPN [figure 2b]. The 0D-LPN has been previously described in detail [8]. A
96 brief outline of the methods is described.

97

98 Heart

99 Right ventricle, and atrial chambers are represented by the time-varying elastance model [3]. Equations
100 1 and 2 describe the pressure-volume relationships of the three cardiac chambers.

101

$$102 \quad 1. \quad a(t) = \begin{cases} \frac{1}{2} \left(1 - \cos \left(\frac{t\pi}{T_{ps}} \right) \right) & 0 < t \leq 2T_{ps} \\ 0 & 2T_{ps} < t \leq T_c \end{cases}$$

103

$$104 \quad 2. \quad P = a(t) \cdot E(V - V_0) + [1 - a(t)] \cdot A(e^{B(V-V_0)} - 1)$$

105

106 $a(t)$ = activation function switching between systole and diastole, E = end systolic elastance, A and B =
107 linear and exponent scaling factor of the end-diastolic pressure-volume relationship respectively, V_0 =
108 unstressed chamber volume, T_c = duration of the cardiac cycle and T_{ps} = time to peak systole. The delay
109 in ventricular systole is accounted for by a temporal translation of Equation (1) by ΔT .

110 The valves are modeled as ideal diodes and an orifice resistance model such that there is no flow when
111 the pressure gradient across the valve is reversed:

112

113 3. $Q = \begin{cases} 0 & \Delta P \leq 0 \\ \sqrt{\frac{\Delta P}{R}} & \Delta P > 0 \end{cases}$

114

115 The atrial septal defect is described as a constant resistance

116

117 Systemic and Pulmonary circulation

118 The circulation was modeled by a multi-compartmental Windkessel method. Each vascular system,

119 pulmonary and systemic, is modeled by a lumped arterial and venous capacitance, and resistance.

120 In each compliant chamber of the circulation, the pressure was determined by assuming a constant

121 compliance:

122

123 4. $P(t) = \frac{V(t)}{C}$

124 Flows were calculated using a linear resistance model:

125

126 5. $Q = \frac{\Delta P}{R}$

127

128

129 The Surgical region

130

131 [1] 0-D Model

132 Symmetry in left and right pulmonary artery flow was assumed in the 0-D model because the same

133 band dimensions were applied to right and left branch PAs during surgery. The pulmonary circulation

134 was therefore modeled as a single unit rather than a left-right lung distribution (figure 2). A reference

135 value R_{ref} was identified using post-hybrid catheterization data and pulmonary flow values were

136 obtained from literature [3]. This reference value was then varied as a function of the external diameter

137 of the PA band (d), adopting a Poiseuille relationship:

138

139 6. $R_{band} = R_{ref} \cdot \left(\frac{3}{d}\right)^4$

140

141

142 Stent flow was described using an empirically derived equation of shunt flow [9] in which the diameter

143 D was scaled to match the pressure difference measured at catheterization:

144

145 7.
$$\Delta P = \frac{k_1 Q + k_2 Q^2}{D^4}$$

146

147 Conservation of Flow

148 The conservation of flow dictates that the change in volume of a compliant chamber must equal

149 the difference of the flow in and out of that specific chamber. This leads to a set of differential

150 equations, which are used to determine a solution. By summing all the individual differential

151 equations for the volume of each compliant chamber it is shown that $\frac{dV_T}{dt} = 0$ where V_T is the total

152 stressed blood volume defined as:

153

154 8.
$$V_T = V_{RA} + V_{RV} + V_{MPA} + V_{SA} + V_{SV} + V_{PA} + V_{PV} + V_{LA}$$

155

156 Thus the total stressed blood volume is a constant and is employed as an input parameter, with the

157 diameters of the band and stent, d and D respectively, to the model to solve the set of ordinary

158 differential equations using Euler's Method.

159

160

161

162 [2] 3-D model

163

164 Using Mimics (Materialize, Leuven, Belgium) a 3-D geometry of the surgical region was constructed

165 from CT scan dataset of patient post-hybrid. Following construction of the geometries the region of the

166 banded areas was manipulated by inserting cylinders of known diameter and length into the banded

167 region and merged into one geometry. The diameter of the cylinders, or virtual bands, was varied under

168 study. Internal meshes were developed in Gambit (Fluent v13, Ansys, Canonsburg, PA) for

169 computational fluid dynamic simulations. Equations (6) and (7) are replaced with the CFD model. The
170 3-D geometry was coupled with the remaining circulation [figure 2b] using the following interface
171 conditions:

172

$$173 \quad 9. \quad Q_{0D} = \int \frac{\dot{m}_i}{\rho} dA_{3D,i}$$

174

$$175 \quad 10. \quad P_{3D,i} = P_{0D}$$

176

177 The Pressure is set from the 0D model, P_{0D} and applied to each face (i) of the boundary in the
178 3D model, $P_{3D,i}$. The CFD model then determines a solution from which the mass flow rate of
179 each face \dot{m}_i is divided by the constant density ρ and integrated over the area of the boundary A
180 to determine the instantaneous volumetric flow rate. [blood density $\rho = 1060 \text{Kg/m}^3$; viscosity $\mu =$
181 $0.005 \text{Kg m}^{-1} \text{s}^{-1}$].

182 With the flows obtained from simulations, oxygen delivery was calculated as previously described by
183 Bove [10]

184

185

186 Protocols

187 Simulations were run in the 3-D model for a range of virtual internal PAB diameters [1.5mm to
188 4.0 mm, 0.5mm increments) with band length = 2 mm. The stent diameter, D , was set at 10mm. For
189 each band size 4 cycles were simulated to converge to a stable solution.

190 The False Position Method was used to determine the value of d_{ext} that corresponded to the equivalent
191 d_{int} simulated in the 3-D model. For comparison between 0-D and 3-D models, two circulation
192 conditions were matched: [1] mean Pulmonary artery pressure and [2] cardiac output.

193

194 Results

195

196 Equivalent external PA band diameters in the 0-D model for each of the six internal diameters 3-D
197 simulations are presented in Table 1. Larger d_{ext} were required to match d_{int} under conditions of

198 matched mean MPA pressure compared to cardiac output. Previous published multiscale simulations
199 identified systemic oxygen delivery was highest with $d_{int} = 2.0$ mm [3,5] which equated to $d_{ext} = 3.1$ mm
200 (matched for CO) or 3.4mm (matched for mean MPA pressure) in the 0-D model.

201 As the internal diameter of PAB increased in the 3D geometries, a decrease in the difference between
202 d_{ext} and d_{int} was observed, particularly at d_{int} 3.5,4mm (figure 4). However, assuming a circular cross-
203 section, the difference between external and internal luminal area, ΔA , remained relatively constant at
204 $\Delta A \approx 4\text{mm}^2$ (figure 4).

205 The overall hemodynamic results, including oxygen delivery and ventricular energetics, for 3D at $d_{int} =$
206 2 mm and the equivalent d_{int} for 0D model are presented in figure 3, table 2. The 3-D and 0-D modeling
207 correlated well with matching for cardiac output producing the closest equivalence.

208

209 Discussion

210

211 Mathematical modeling has the potential to inform surgical decision-making and optimize the Hybrid
212 procedure in HLHS. With the multiscale approach 3-D patient-specific geometries of the surgical
213 region are constructed, and hemodynamic profiles determined by computational fluid dynamics. This
214 provides an analysis of the Hybrid circulation but long computational times limits clinical application.
215 Alternatively a simpler equation-based 0-D model incorporating external stent and PA band diameters
216 is computer efficient and could provide rapid clinical applicable solutions.

217 This study compared the 0-D and 3-D models, and determined the external PA band diameters of the
218 0D model that corresponded to a range of internal diameters simulated in the 3D model. The difference
219 in diameter between equivalent internal and external band dimensions was not consistent but varied
220 over the band range. Potentially this was due to the minor degrees of alignment error associated with
221 insertion of the virtual bands within the 3-D geometries.

222 Ideal hybrid palliation aims to maximize systemic oxygen delivery within the workload capacity of the
223 single ventricle by optimizing $Q_p:Q_s$. by PAB calibration.[2,7]. Previous studies have demonstrated an
224 internal diameter of 2 mm provides the optimum systemic oxygen delivery for a 3kg neonate [4,6]. In
225 this study 2 mm internal PAB diameter [3-D model] corresponded to an external diameter of 3.1/3.4
226 mm in the 0-D model. This finding is consistent with that observed clinically in which 3-3.5 mm is the
227 typical external band diameter applied in 3kg neonate.

228

229 The study further demonstrated that 0-D and 3-D models, with matched boundary conditions and
230 corresponding PA band dimensions, demonstrated equivalent ventricular energetics and hemodynamic
231 outcomes.

232 The implications of the study are two-fold. Firstly, the study confirms that in comparison with 3D-
233 multiscale modeling, the 0-D approach can provide a valid representation of the hybrid circulation.
234 Secondly, there is the potential for 0-D and 3-D models to be used interchangeably to inform clinical
235 management. Initial patient-specific 3-D geometry with virtual internal PA band and stent dimension
236 calibration can be used to define the optimal hemodynamics for the individual patient's anatomy. The
237 corresponding external PA band diameter, as determined by this study, can be applied to configure the
238 hybrid procedure and also used to input the 0-D model. Any subsequent circulation analyses [e.g. due
239 to subsequent stent obstruction] could be evaluated via the efficient 0-D model.

240 In conclusion the study compared two modeling approaches, 0-D and 3-D in the computational analysis
241 of the hybrid palliation of HLHS. The models demonstrated close equivalence of predicted
242 hemodynamics. Internal PA band diameter of 2 mm corresponded to external band diameter of 3.1/3.4
243 mm in the 0D model, consistent with clinical observation. From this study we conclude that 0-D
244 modeling can provide a valid clinically applicable alternative to 3D-multiscale in the Hybrid-HLHS
245 circulation.

246

247 Funding: Department of Bioengineering, University of Strathclyde, Glasgow.

248 Ethics: Caldicott Guardian, West of Scotland Ethics Committee.

249 Conflict of Interest: None

250

251

252

253

254

255

256

257

258 References

259

260 1. Galantowicz M, Cheatham JP, Phillips A, Cua CL, Hoffman TM, Hill SL, Rodeman R. Hybrid
261 approach for hypoplastic left heart syndrome: intermediate results after the learning curve. *Ann Thorac*
262 *Surg* 2008;85:2063-71

263

264 2. Kitahori K, Murakami A, Takaoka T, Takamoto S, Ono M. precise evaluation of bilateral pulmonary
265 artery banding for initial palliation in high-risk hypoplastic left heart syndrome. *J Thorac Cardiovasc*
266 *Surg* 2010;140:1084-91

267

268 3. Shimizu S, Une D, Shishido T, Kamiya A, Kawada T, Sano S, Sugimachi. Norwood procedure with
269 non-valved right ventricle to pulmonary artery shunt improves ventricular energetics despite the
270 presence of diastolic regurgitation: a theoretical analysis. *J Physiol Sci* 2011;61:457-65

271

272 4. Corsini C, Cosentino D, Pennati G, Dubini G, Hsia TY, Migliavacca F. Multiscale models of the
273 hybrid palliation for hypoplastic left heart syndrome. *Journal of Biomechanics* 2011;44:767-70

274

275 5. Hsia TY, Cosentino D, Corsini C, Pennati G, Migliavacca F. Use of mathematical modeling to
276 compare and predict haemodynamic effects between hybrid and surgical Norwood palliations for
277 hypoplastic left heart syndrome. *Circulation* 2011; 124:S204-10

278

279 6. Baker CE, Corsini C, Cosentino D, Dubini G, Pennati G, Migliavacca F, Hsia TY. Effects of
280 pulmonary artery banding and retrograde arch obstruction on the hybrid palliation of hypoplastic left
281 heart syndrome. *J Thorac Cardiovasc Surg* 2013;146:1341-8

282

283 7. Ceballos A, Argueta-Morales R, Divo E, Osorio R, Calderone CA, Kassab AJ, DeCampi WM.
284 Computational Analysis of Hybrid Norwood Circulation with Distal Aortic Arch Obstruction and
285 Reverse Blalock-Taussig Shunt. *Ann Thorac Surg* 2012;94:1540-50

286

- 287 8. Young A, Gourlay T, McKee S, Danton MH. Computational modeling to optimize the hybrid
288 configuration for hypoplastic left heart syndrome. *Eur J Cardiothorac Surg*, 2013 Oct;44(4):664-72
289
- 290 9. Migliavaccaa, F, Yates R, Pennati G, Dubini G, Fumero R., de Leval MR. Calculating blood flow
291 from Doppler measurements in the systemic-to-pulmonary artery shunt after the Norwood operation: A
292 method based on computational fluid dynamic. *Ultrasound in Med & Biol* 2000;26(2):209-219
293
- 294 10. Bove EL, Migliavacca F, de Leval MR, Balossino R, Pennati G, Lloyd TR, Khambadkone S, Hsia,
295 TY, Dubini G. Use of mathematic modeling to compare and predict hemodynamic effects of the
296 modified blalock-taussig and right ventricle-pulmonary artery shunts for hypoplastic left heart
297 syndrome. *J Thorac Cardiovasc Surg* 2008; 136:312 – 320

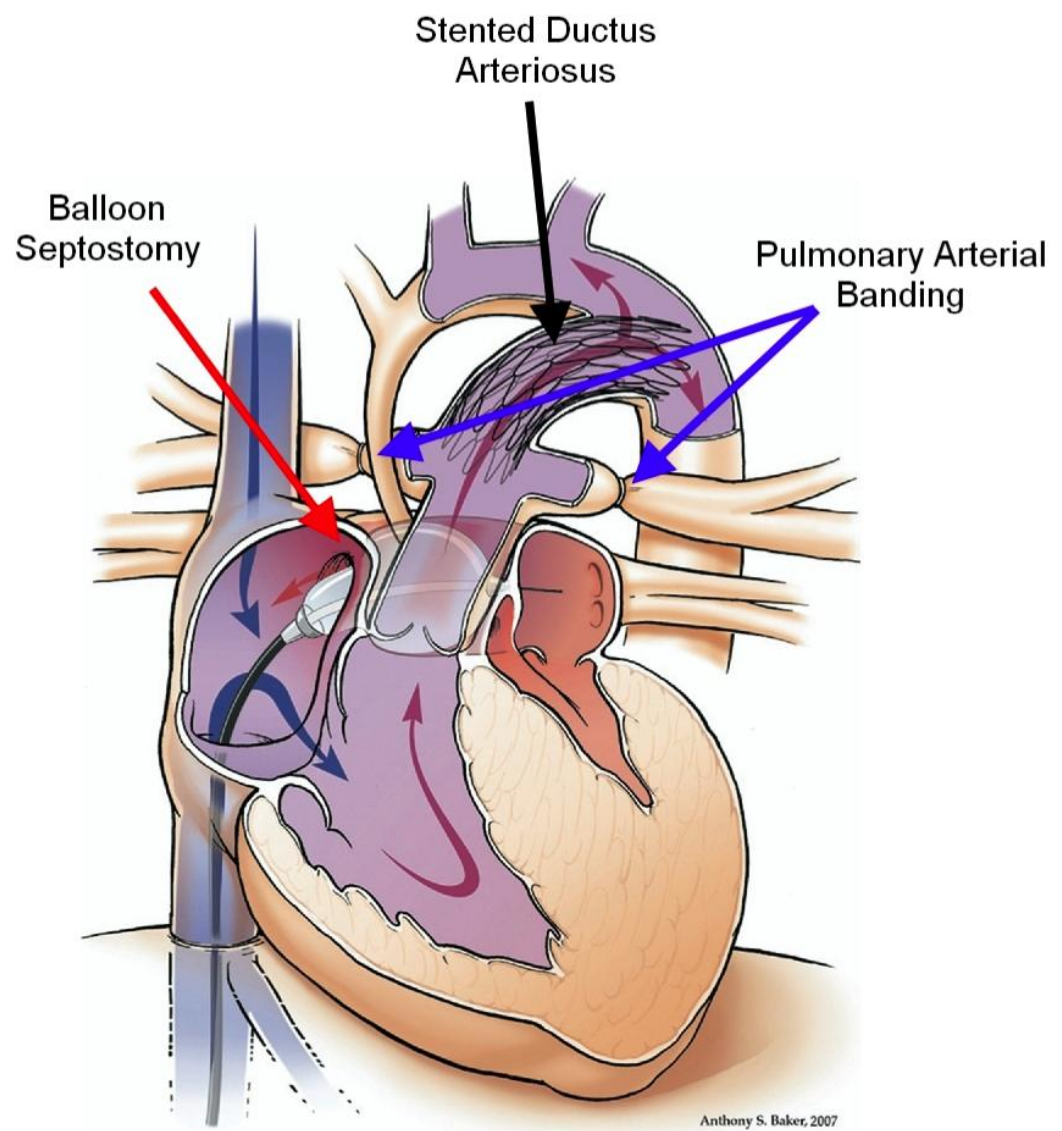
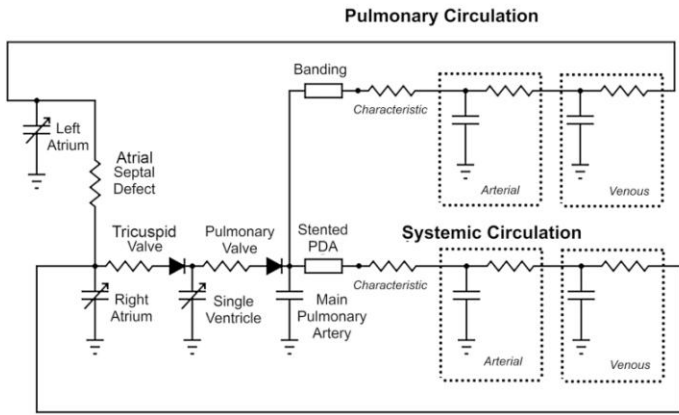
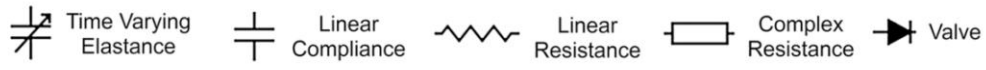
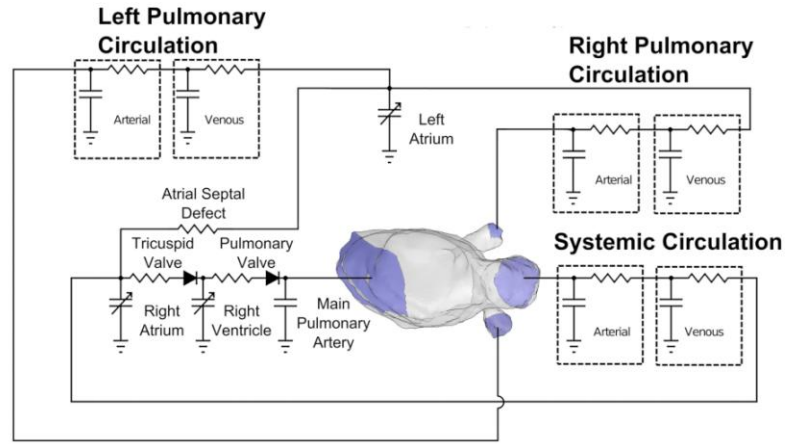


figure 1. Illustration of the Hybrid procedure reprinted from Galantowicz et al [1] reproduced with author's permission

Figure 2. Analogous electric circuit diagrams of zero-dimensional and 3D-multiscale models



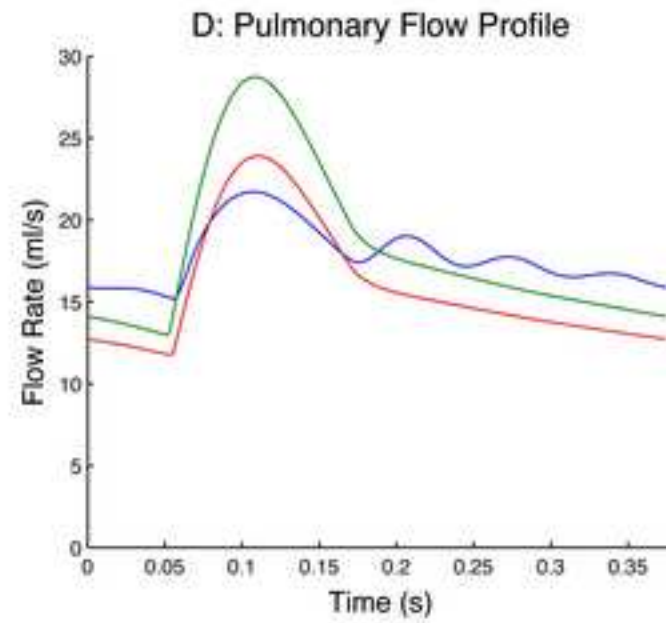
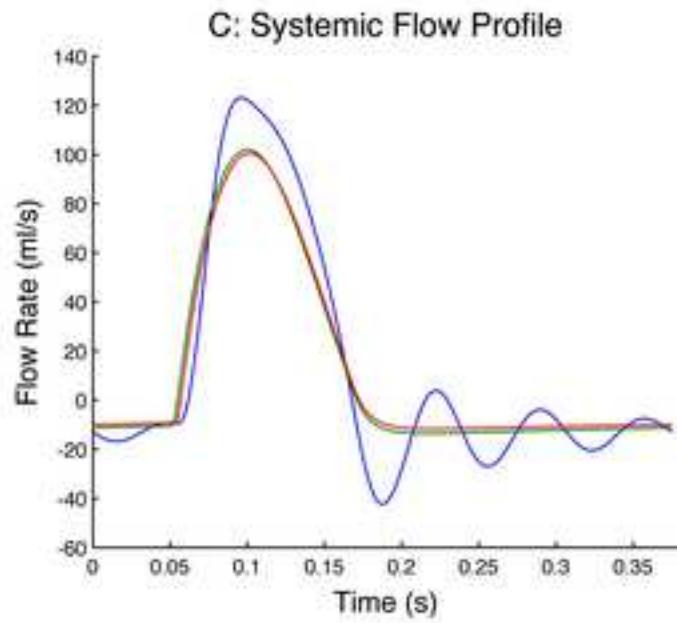
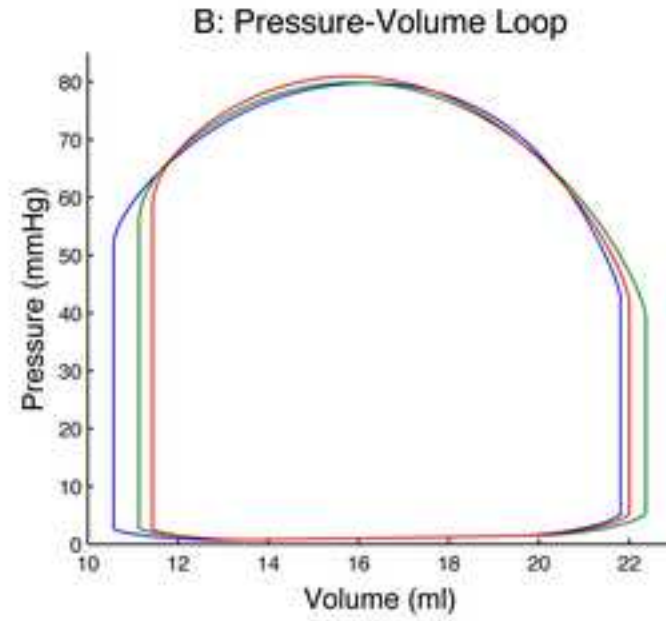
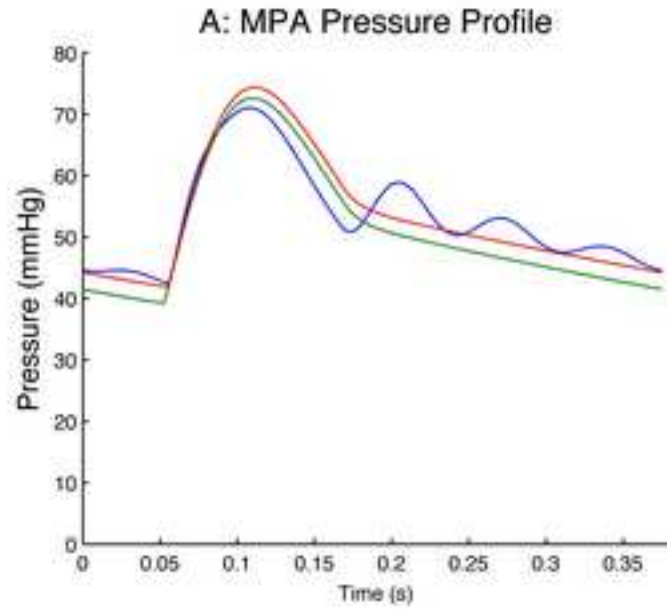
(a) Zero dimensional



(b) Multiscale

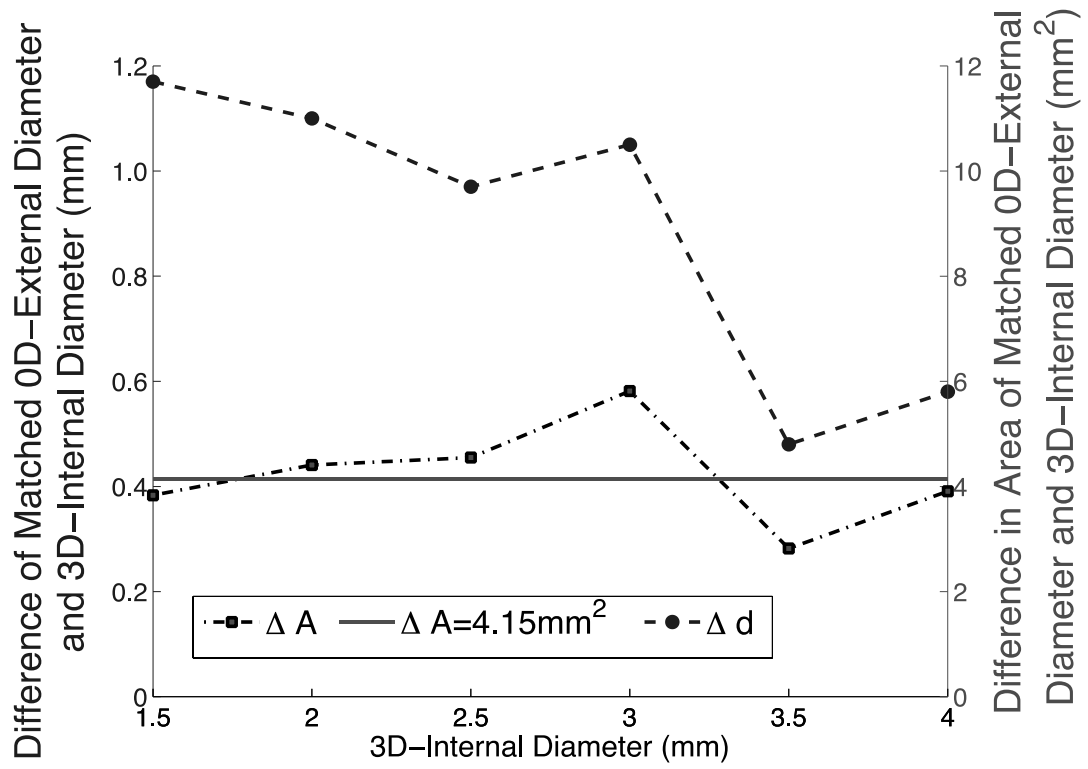
Figure

[Click here to download high resolution image](#)



— 3D Model — 0D Model Matched for Cardiac Output — 0D Model Matched Mean MPA Pressure

Figure 4. Difference in diameter and area of OD-external versus 3D-internal pulmonary artery band dimensions, matched for cardiac output



3D Diameter	0D Diameter to match cardiac output	0D Diameter to match MMPA pressure
1.5 mm	2.67 mm	2.97 mm
2.0 mm	3.10 mm	3.40 mm
2.5 mm	3.47 mm	3.81 mm
3.0 mm	4.05 mm	4.55 mm
3.5 mm	3.98 mm	4.45 mm
4.0 mm	4.58 mm	5.37 mm

Table 1. Equivalent external band diameter of 0-D model for internal band diameter in 3-D model when matched for cardiac output and mean MPA pressure.

Outcome	3D model	0D model matching MPA pressure	0D model matching cardiac output
Band Diameter (mm)	2.00	3.40	3.10
Systolic MPA Pressure (mmHg)	71.04	77.86, 8.7%	80.31, 11%
Diastolic MPA Pressure (mmHg)	42.42	40.25, 5.1%	44.55, 2.5%
Mean MPA Pressure (mmHg)	53.41	53.41	57.08, 6.4%
Systolic Systemic Pressure (mmHg)	58.80	73.24, 19.7%	75.98, 22.6%
Diastolic Systemic Pressure (mmHg)	42.53	40.31, 5.2%	44.60, 4.6%
Mean Systemic Pressure (mmHg)	50.31	52.73, 4.5%	56.43, 10.8%
Systolic Pulmonary Pressure (mmHg)	14.50	17.68, 17.9%	14.40, 0.6%
Diastolic Pulmonary Pressure (mmHg)	13.17	14.37, 8.3%	12.08, 8.2%
Mean Pulmonary Pressure (mmHg)	13.91	16.10, 13.6%	13.29, 4.4%
Cardiac Output (l/min)	1.80	1.98, 9%	1.80
Pulmonary Flow (l/min)	1.07	1.24, 13.7%	1.00, 6.5%
Systemic Flow (l/min)	0.73	0.74, 1%	0.79, 7.5%
Pulmonary-Systemic Flow Ratio	1.47	1.68, 12.5%	1.27, 13.6%
Stent Backflow (l/min)	-0.64	-0.55, 14%	-0.45, 29%
Arterial Oxygen Saturation (%)	72.22	75.77, 4.6%	70.54, 2.3%
Venous Oxygen Saturation (%)	34.35	38.32, 10%	35.76, 3.9%
Systemic Oxygen Delivery (ml O ₂ /min/m ²)	352.77	374.30, 5.7%	375.23, 5.9%
Total Stressed Blood Volume (ml)	72.50	72.50	72.50
Right Ventricle End Diastolic Volume (ml)	21.81	23.62, 7.6%	22.99, 5.1%
Stroke Work (ml · mmHg)	782.87	833.78, 6.1%	791.44, 1%
Systolic Pressure-Volume Area (ml · mmHg)	962.98	1057.87, 8.9%	1045.77, 7.9%
Mechanical Efficiency (%)	81.30	78.82, 3%	75.68, 6.9%

Table 2. Haemodynamic outcomes of 3D versus OD models with equivalent pulmonary artery band dimensions when matched for mean MPA pressure and cardiac output, with % difference between 3D and OD outputs